Mitsui *Earth, Planets and Space (2018) 70:136*
https://doi.org/10.1186/s40623-018-0911-8

Earth, Planets and Space

FULL PAPER

Open Access

Elastic interaction of parallel rate-and-state-dependent frictional faults with aging and slip laws: slow-slip faults can sometimes host fast events

Yuta Mitsui*

Abstract

In contrast to surface observation of complex earthquake faults, simple fault-plane models are frequently sufficient to fit geophysical data of seismic wave or crustal deformation. However, earthquake occurrence should be strongly affected by fault interaction between separate faults. To understand its mechanics, rate-and-state frictional models of separate faults within elastic continuum would be important. We construct a conceptual out-of-plane model of aligned parallel faults (causing stress shadows) in a two-dimensional elastic body, assuming both "aging" and "slip" type of state evolution laws. We find that close fault conditions (roughly for smaller inter-fault distance than fault length) favor higher-speed slip events than distant fault conditions. In a practical sense, the elastic interaction only affects faults that are hosting slow events. This point does not depend on the state evolution laws (aging or slip). Our result implies that the parallel distribution of the frictional faults contributes occurrence of relatively fast slip in a slow-slip region.

Keywords: Fault slip, Elastic interaction, Parallel fault, Rate-and-state friction, Aging law, Slip law

Introduction

Many researches have constructed physical models of interseismic, coseismic, and post-seismic fault slip behavior. In particular, frictional models assuming a rate-and-state-dependent law (Dieterich 1979; Ruina 1983) within elastic continuum have succeeded in representing long-term stick–slip behavior (both fast and slow slips) with spontaneous nucleation (Tse and Rice 1986, and following studies). Such a model has been developed mainly for investigating effects elastic interaction between multiple focal areas of slip events on a straight or curved fault plane (e.g., Kato 2004; Hori 2006; Veedu and Barbot 2016; Li and Liu 2016), due to computational costs. Investigation of elastic interaction of separate faults has been limited to each phase of static (e.g., King et al. 1994) and dynamic (e.g., Harris and Day 1993) slips.

Simple fault-plane models in an elastic body are frequently enough to fit geophysical data of seismic wave or crustal deformation (Aki and Richards 2002; Segall 2010; Veedu and Barbot 2016), in contrast to surface observation for complex faults (e.g., Ujiie and Kimura 2014). However, earthquake occurrence may be strongly affected by fault interaction, as inferred from several discrete (not elastic continuum) models (e.g., Carlson and Langer 1989; Bak and Tang 1989). Rate-and-state frictional models of complex faults within elastic continuum would be important for understanding mechanics of earthquake occurrence.

One previous study (Kato and Hirasawa 2000) investigated interaction of separate rate-and-state faults for a specific case of a plate subduction zone. A recent study (Romanet et al. 2018) showed that two overlapping (parallel) rate-and-state faults lead to a complex stick–slip

*Correspondence: mit@shizuoka.ac.jp
Department Geosciences, Shizuoka University, 836, Ohya, Suruga-ku, Shizuoka 422-8529, Japan

behavior. These pioneer studies illuminated the importance of geometrical complexity.

Here, we point out that the previous studies assumed the "aging" type of state evolution law only. Since the aging law well represents time-dependent frictional healing (Dieterich and Kilgore 1994), recent studies revealed that another "slip" type of state evolution law better fit both velocity-step experiments and slide-hold-slide experiments (Bhattacharya et al. 2017). Thus, we should also investigate cases of the slip law. Nucleation processes of stick slips on the "aging law" fault and "slip law" faults are quantitatively different even without fault interaction (e.g., Ampuero and Rubin 2008; Rubin 2008; Mitsui and Hirahara 2011). In particular, parameter ranges for spontaneous slow slips of the two evolution laws are evidently different. Using only one side may lead to misunderstandings of earthquake generation mechanism.

This study illuminates the role of elastic interaction between separate rate-and-state faults with the aging and slip evolution law. We especially focus on maximal slip velocities as an index of elastic effects between separate faults.

Materials and methods

Frictional fault model

We revise a shear fault model in our previous study (Mitsui et al. 2012) and construct a conceptual model of parallel faults in a two-dimensional elastic body, which is similar to the model of Romanet et al. (2018), but two points are different other than the state evolution law. One different point is the fault geometry. We assume aligned parallel faults as shown in Fig. 1 for simplicity. The other point is a loading system. We do not assume uniform stress loading but that through slip deficits from steady slip following many previous studies (e.g., Tse and Rice 1986; Rubin 2008; Mitsui and Hirahara 2011). Namely, the loading shear stress τ at a numerically discretized grid X_i is given by

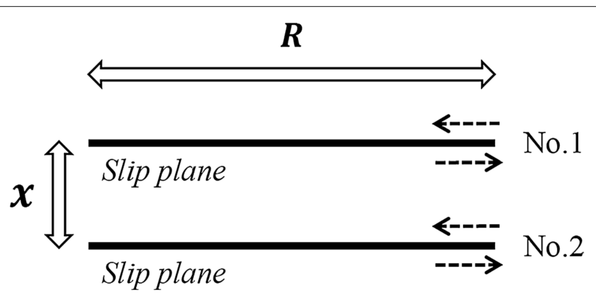

Fig. 1 Parallel fault model in this study. Two shear faults (No. 1 & 2) of length *R* are set at a distance of *x*, and not overlapped

$$\tau(X_i) = \tau_0 + \sum_{X_j} K\left(X_i - X_j\right)\left[v_0 t - u\left(X_j\right)\right] \tag{1}$$

t is elapsed time, v_0 is background slip rate (1 mm/yr in this study), and u is slip amount. Elastic stiffness kernel K is calculated on the basis of the Green's function in a homogeneous elastic half-space (Rani and Singh 1992), where the model faults are sufficiently distant from the free surface. In order to avoid stress singularities, we lay the discretized grids for τ and u in a staggered pattern.

The loading shear stress τ at each grid is related to friction τ_f by quasi-static equilibrium with S-wave radiation damping (Rice 1993):

$$\tau - \frac{Gv}{2c_s} = \tau_f \tag{2}$$

where G is rigidity (32 GPa in this study), v is slip rate, and c_s is S-wave velocity (3464 m/s in this study). Moreover, the friction τ_f is composed of effective normal stress $\bar{\sigma}$ (50 MPa in this study) and frictional coefficient μ.

Finally, the frictional coefficient μ changes obeying the rate-and-state-dependent law (Dieterich 1979; Ruina 1983). It depends on the slip rate v and a state variable θ as follows:

$$\mu = \mu_0 + a\ln\left(\frac{v}{v_0}\right) + b\ln\left(\frac{\theta}{L/v_0}\right) \tag{3}$$

a, b, L are controlling parameters. If $a - b < 0$, the frictional fault has rate-weakening behavior. The state variable θ evolves following the aging law or slip law. The aging law is

$$\frac{d\theta}{dt} = 1 - \frac{v\theta}{L}, \tag{4}$$

and the slip law is

$$\frac{d\theta}{dt} = -\frac{v\theta}{L}\ln\left(\frac{v\theta}{L}\right) \tag{5}$$

Table 1 Frictional parameters in this study

Case	a	b	L [μm]	R/L_{b-a}	R/L_b	h/h^*
1	0.015	0.02	2.5	6.24	25.0	0.049
2	0.015	0.02	5.0	3.12	12.5	0.025
3	0.015	0.02	10	1.56	6.24	0.012
4	0.005	0.02	10	4.68	6.24	0.037
5	0.01	0.02	20	1.56	3.12	0.012

For both evolution laws, smaller L destabilizes the frictional fault via rapid state evolution.

In our numerical calculations, each fault is discretized into 200 grids. We confirmed that the grid size h is less than 1/10 of a certain critical size "h^*" within the framework of the continuum limit (Rice 1993) using frictional parameters described in the following section (Table 1).

As initial conditions, we set $\theta = L/(0.9v_0)$ on Fault 1 and $\theta = L/(1.1v_0)$ on Fault 2, respectively, with $v = v_0$ for the entire grid. On the basis of the RK45 algorithm (Press et al. 1992), we simultaneously solve the above equation after differentiating Eqs. (1)–(3) with time (thus τ_0 and μ_0 are vanished).

Parameters

We note that the calculation results from the above system can be scaled with spatial distance, except for the effect of the S-wave radiation damping term which is small for earthquake nucleation processes (see Mitsui and Hirahara 2011). Therefore, we decided to fix the fault length $R = 2$ m and vary the ratio of x/R in a range from 0.05 to 5 for numerical experiments. We do not assume too small x/R, because the discretized grid size divided by R is $1/200 = 0.005$.

For frictional parameters, we first fix $a = 0.015$, $b = 0.02$ and vary L (Cases 1–3). Next, from Case 3, we change two non-dimensional parameters as Case 4 and Case 5: R/L_{b-a} and R/L_b, where L_{b-a} is given by $L_{b-a} = GL/(\bar{\sigma}(b-a))$ and $L_b = GL/(\bar{\sigma}b)$. The former (L_{b-a}) is related to a characteristic nucleation size "h^*" in traditional studies (e.g., Rice 1993), and the latter (L_b) may also control nucleation (e.g., Dieterich 1992), for example, creep speed in an early nucleation phase (Mitsui and Hirahara 2011). Note that Romanet et al. (2018) used a parameter in proportion to $L_{b-a}(b/(b-a))$ or $L_b(b/(b-a))^2$. Because this parameter has a meaning only for the aging law with crack-like nucleation (Rubin and Ampuero 2005; Rubin 2008; Mitsui and Hirahara 2011), we do not use this parameter.

Table 1 summarizes the parameters in this study. For each Case of 1–5, we test various x/R in the range from 0.05 to 5 and both aging and slip state evolution laws.

Results

As a typical result of the fault interaction, Fig. 2 shows spatiotemporal evolution of the slip rate $\log(v/v_0)$ and the frictional coefficient μ during multiple stick–slip sequence, in Case 2 with the aging law. For a single fault (Fig. 2a), periodic slow stick–slips occur. The friction (normalized shear stress by normal stress) evolution shows inward creep from the fault edges within interseismic periods. By contrast, the parallel fault model (Fig. 2b) exhibits non-periodic stick–slip behavior. Moreover, several-orders faster slip event (large $\log(v/v_0)$) occurs in the parallel fault model (Fig. 2b).

In order to check the elastic interaction, Fig. 3 shows temporal evolution of the slip rate $\log(v/v_0)$ at the fault centers in Case 2 with the aging law (same as Fig. 2). We easily expect that smaller x/R leads to stronger elastic interaction between the faults. In the distant faults case ($x/R = 0.5$), the periodic (regular) stick slip has simply occurred on the faults (Faults 1 & 2). By contrast, in the close faults case ($x/R = 0.05$), the periodicity spontaneously breaks and irregular slip events continue for a certain period. During the irregular periods, several-orders faster slip events (large $\log(v/v_0)$) occur, as Fig. 2b.

An enlarged graph of Fig. 3b is useful to see the details of the elastic interaction (Fig. 4). We find that slip events on one fault instantaneously decrease slip rates of the other fault. Fast-slip events on both faults do not synchronize at the same time. This is because of stress shadows beside dislocations (e.g., Harris and Simpson 1998).

Next, in order to systematically investigate effects of the inter-fault distance x/R, we focus on the maximum slip rates and recurrence intervals. Figure 5 shows the maximum slip rates and the recurrence intervals during the multiple stick–slip sequences for various x/R, in Case 2 with the aging law (as Figs. 2, 3, and 4). Figure 5a exhibits that the maximum slip rate increases by several orders of magnitude, and simultaneously, Fig. 5b reveals that the event recurrence intervals are fluctuated, approximately for smaller x/R than 1.

Finally, we show the calculation results of all the cases (Table 1) in Fig. 6. We find that close fault conditions (approximately for smaller x/R than 1) tend to have higher slip rates than distant fault conditions (nearly equal to single fault conditions), when the distant fault conditions have sufficiently low slip rates ($< 10^{-5}$ m/s). This tendency indicates that the elastic interaction affects "originally slow-slip faults" but does not affect "originally fast-slip faults," practically.

Discussion

Figure 6 shows that the elastic interaction only affects faults that are hosting slow events. This point does not depend on the state evolution laws (aging or slip) although the calculation results themselves strongly

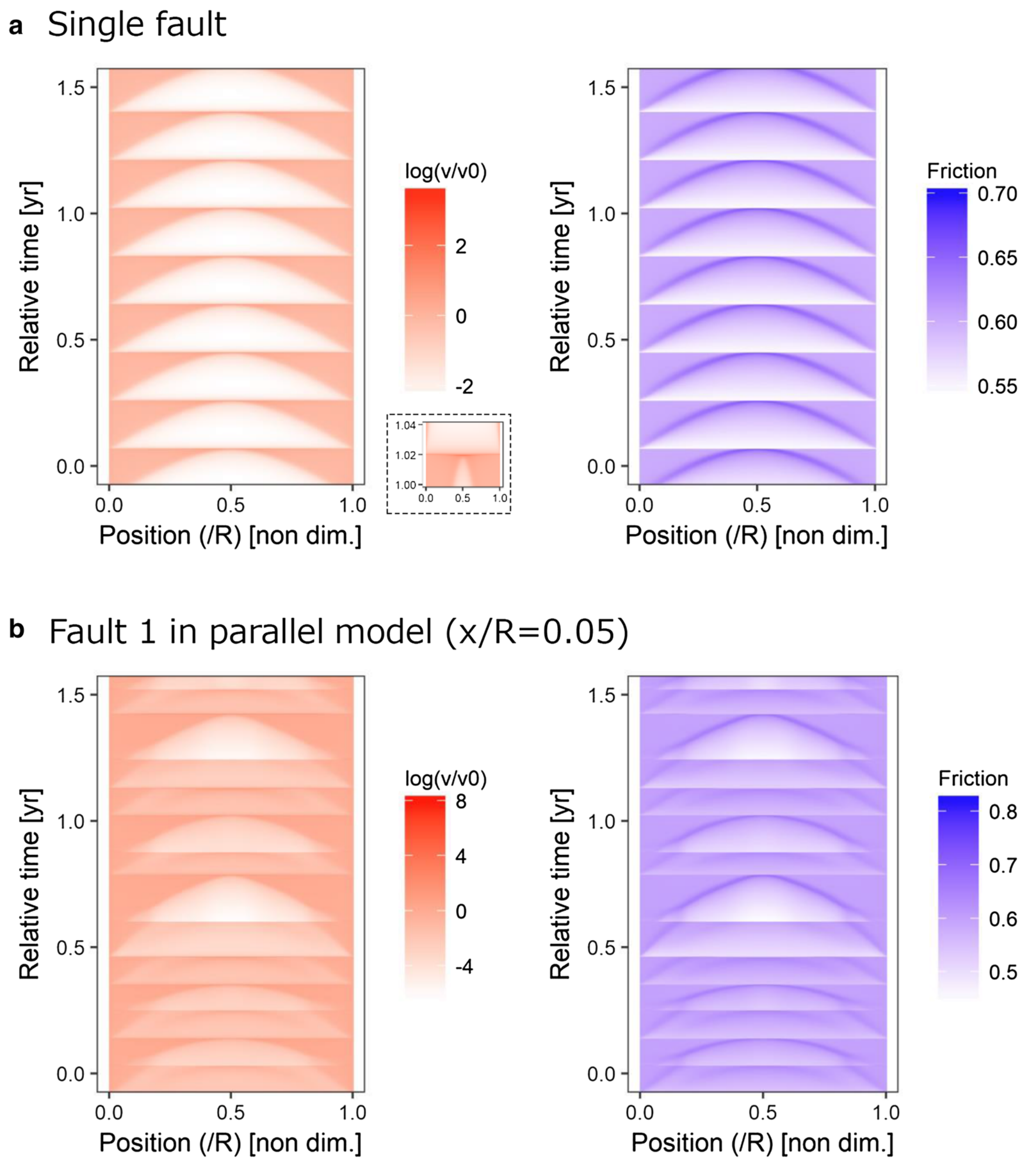

Fig. 2 Spatiotemporal evolution of the common logarithmic slip rate log(v/v_0) and the frictional coefficient μ during multiple stick–slip sequence, in Case 2 with the aging law. The horizontal axes are normalized fault position, and the vertical axes are relative time. We show the calculation results after many slip events from the initial condition. **a** In case of the single fault. A small figure surrounded by a dotted line represents an enlarged graph around one slip event. **b** In case of Fault 1 of the parallel model with $x/R = 0.05$

depend on the state evolution laws (for example, Case 2 and Case 5 of the frictional parameters). In order to check the mechanism of the fast-slip event on "originally slow-slip faults" is the same between the aging and slip state evolution laws, Fig. 7 exhibits the spatiotemporal evolution of the slip rate log(v/v_0) in Case 5 with the slip law. In contrast to the periodic slow events of the single fault model in Fig. 7a, far-faster slip events

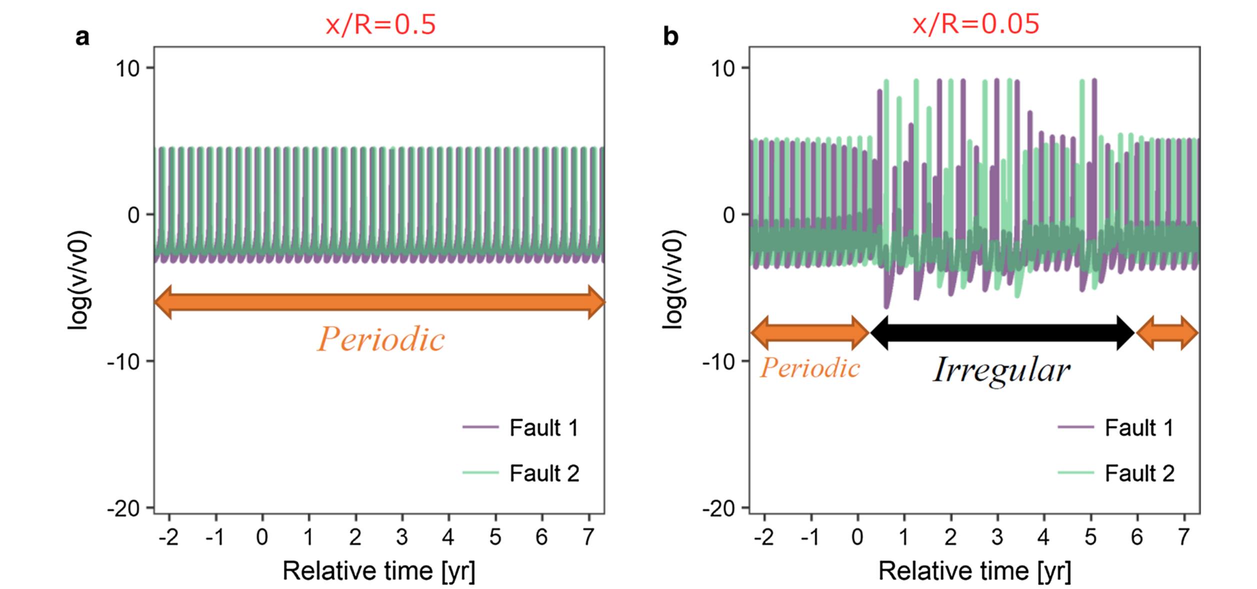

Fig. 3 Temporal evolution of the common logarithmic slip rate $\log(v/v_0)$ at the fault centers during multiple stick–slip sequence, in Case 2 with the aging law (same as Fig. 2). **a** In case of $x/R = 0.5$. **b** In case of $x/R = 0.05$

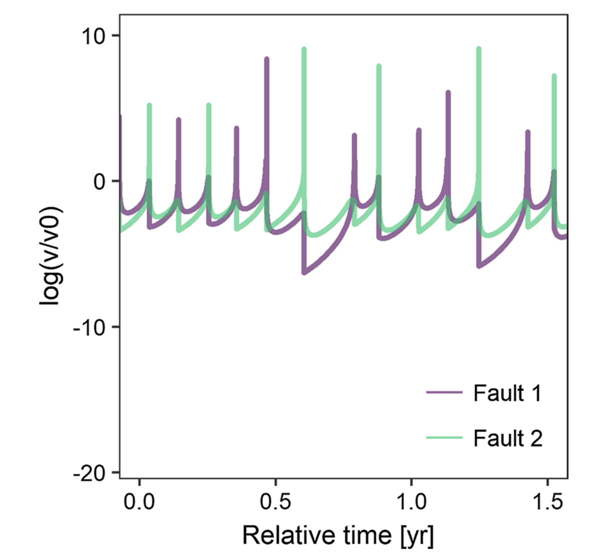

Fig. 4 Temporal evolution of the common logarithmic slip rate $\log(v/v_0)$ at the fault centers for the same setting as Fig. 3b of $x/R = 0.05$, during the irregular phase

occur on the parallel fault model of Fig. 7b. From Fig. 7b, we can see that the fault slip rates of Fault 1 are strongly decreased by the fast slips on the other fault (Fault 2). The first decrease may trigger the following fast slip on Fault 1, but the second decrease does not directly cause the fast slip. As above, the details of the frictional responses due to the elastic interaction are rather complex.

Our finding of the promotion effects of the elastic fault interaction on the fault slip rates is not trivial, because slips of the parallel faults cause negative static stress changes for each other that lead to slip restraints in the classical concept (stress shadows). The numerical modeling of the rate-and-state frictional faults within elastic continuum has contributed to this finding. Nucleation characteristics on rate-and-state faults are not simple. For instance, positive stress change does not always lead to early event occurrence and negative stress change does not always lead to late event occurrence (Kaneko and Lapusta 2008; Cho et al. 2009). In addition, large stress

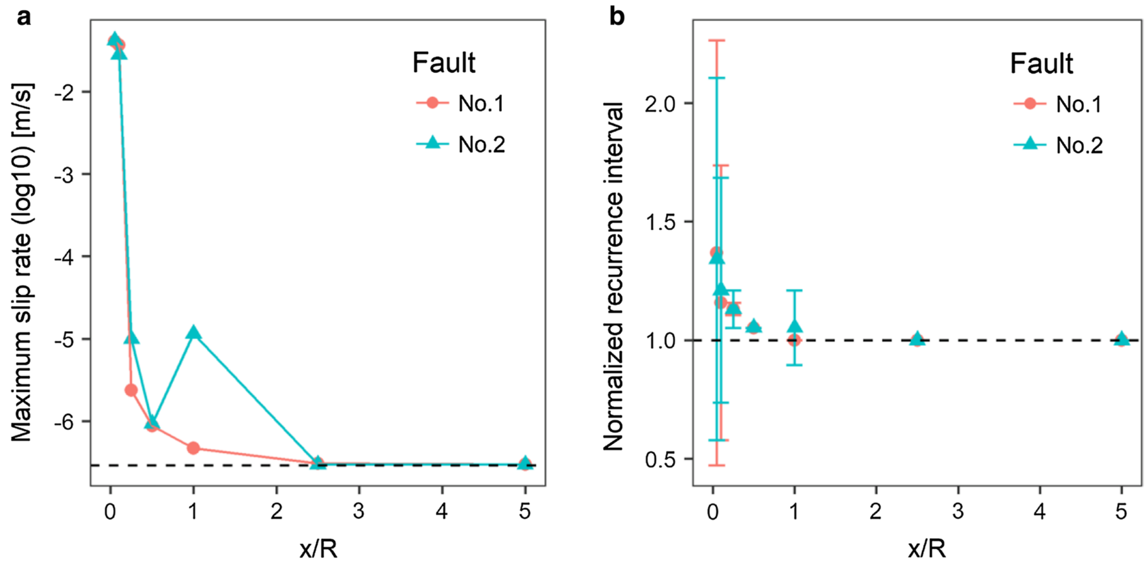

Fig. 5 Effects of the inter-fault distance *x/R* in Case 2 with the aging law. **a** Maximum slip rates at the fault centers. The horizontal broken line means the result for a single fault. **b** Event recurrence intervals normalized by that for a single fault (horizontal broken line). The vertical bars represent fluctuation ranges

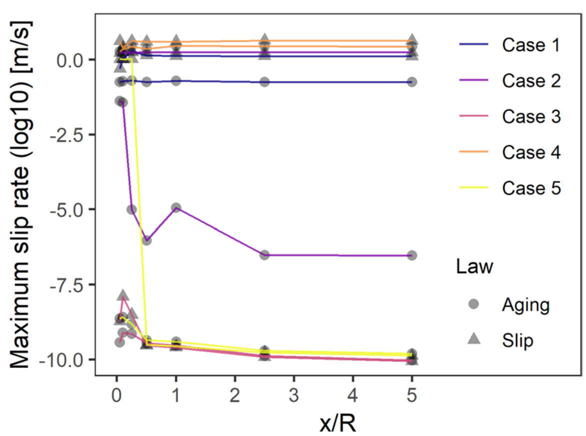

Fig. 6 Maximum slip rates (for both Faults 1 and 2) at the fault centers. The color lines represent the cases of the frictional parameters (Table 1), and the markers represent the state evolution laws of the rate-and-state-dependent friction

changes on rate-and-state faults can cause complicated long-term responses (Mitsui 2015) which have not been well investigated. Besides, dynamic elastic interaction among seismic wave and faults may further promote fault slip via dynamic triggering (Harris and Day 1993).

A geological observation study (Fagereng et al. 2011) proposed that incrementally developed (parallel) slip surfaces, found in an accretionary mélange, are records of episodic tremor and slow-slip events. The parallel fault distribution might contribute occurrence of observable episodic tremor (relatively fast slip) in a slow-slip region (e.g., Nakano et al. 2018).

Conclusions

Our numerical modeling of separate rate-and-state faults with the aging and slip evolution law revealed that the elastic interaction between parallel faults (mainly

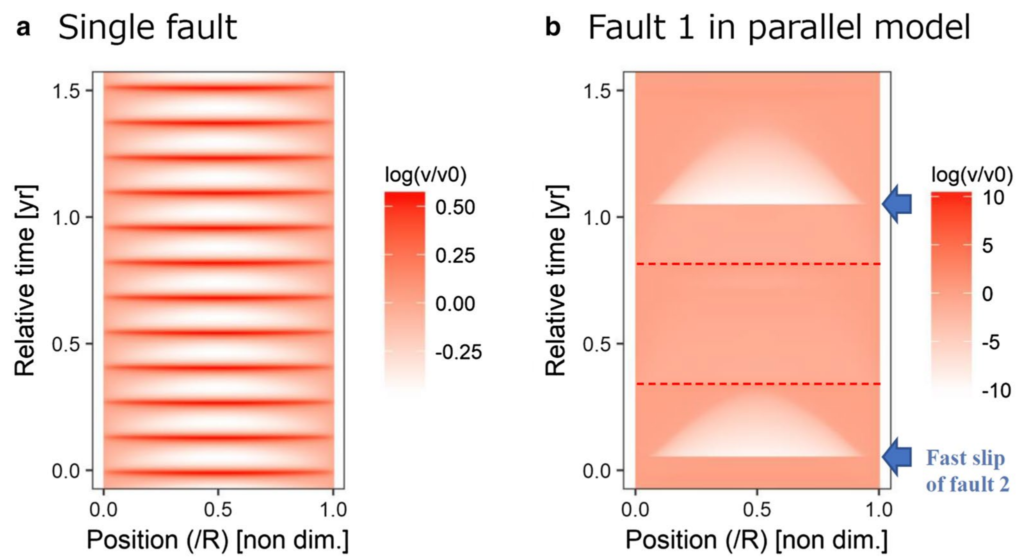

Fig. 7 Spatiotemporal evolution of the common logarithmic slip rate log(v/v_0) during multiple stick-slip sequence, in Case 5 with the slip law. **a** In case of the single fault. **b** In case of Fault 1 of the parallel model with $x/R = 0.1$. The red and broken horizontal lines represent the time of fast-slip events, and the blue arrows represent the time of fast-slip events of the other fault (Fault 2)

negative stress change) favors higher-speed slip events. This tendency does not depend on the state evolution laws.

Authors' contributions
YM performed the numerical experiments and wrote the paper. The author read and approved the final manuscript.

Acknowledgements
The author acknowledges anonymous reviewers for their constructive reviews.

Competing interests
The author declares that he has no competing interests.

Availability of data and materials
Please contact the author for data requests.

Funding
This study was supported by the Japan Society for the Promotion of Science (JSPS) KAKENHI, Grant Numbers JP16K17791 and JP16H06477.

Publisher's Note
Springer Nature remains neutral with regard to jurisdictional claims in published maps and institutional affiliations.

Received: 26 April 2018 Accepted: 16 August 2018
Published online: 22 August 2018

References
Aki K, Richards P (2002) Quantitative seismology, 2nd edn. University Science Books, Sausalito
Ampuero J-P, Rubin AM (2008) Earthquake nucleation on rate and state faults—aging and slip laws. J Geophys Res 113:B01302. https://doi.org/10.1029/2007JB005082
Bak P, Tang C (1989) Earthquakes as a self-organized critical phenomenon. J Geophys Res 94:15635–15637. https://doi.org/10.1029/JB094iB11p15635
Bhattacharya P, Rubin AM, Beeler NM (2017) Does fault strengthening in laboratory rock friction experiments really depend primarily upon time and not slip? J Geophys Res 122:6389–6430. https://doi.org/10.1002/2017JB013936
Carlson J, Langer J (1989) Properties of earthquakes generated by fault dynamics. Phys Rev Lett 62:2632–2635. https://doi.org/10.1103/PhysRevLett.62.2632
Cho I, Tada T, Kuwahara Y (2009) Stress triggering of large earthquakes complicated by transient aseismic slip episodes. J Geophys Res 114:B07310. https://doi.org/10.1029/2008JB006125
Dieterich JH (1979) Modeling of rock friction 1. Experimental results and constitutive equations. J Geophys Res 84:2161–2168. https://doi.org/10.1029/JB084iB05p02161
Dieterich JH (1992) Earthquake nucleation on faults with rate-and state-dependent strength. Tectonophysics 211:115–134. https://doi.org/10.1016/0040-1951(92)90055-B
Dieterich JH, Kilgore BD (1994) Direct observation of frictional contacts: new insights for state-dependent properties. Pure Appl Geophys 143:283–302. https://doi.org/10.1007/BF00874332
Fagereng Å, Remitti F, Sibson RH (2011) Incrementally developed slickenfibers—Geological record of repeating low stress-drop seismic events? Tectonophysics 510:381–386. https://doi.org/10.1016/j.tecto.2011.08.015
Harris RA, Day M (1993) Dynamics of fault interaction: parallel strike-slip faults. J Geophys Res 98:4461–4472. https://doi.org/10.1029/92JB02272
Harris RA, Simpson RW (1998) Suppression of large earthquakes by stress shadows: a comparison of Coulomb and rate-and-state failure. J Geophys Res 103:24439–24451. https://doi.org/10.1029/98JB00793
Hori T (2006) Mechanisms of separation of rupture area and variation in time interval and size of great earthquakes along the Nankai Trough, southwest Japan. J Earth Simul 5:8–19
Kaneko Y, Lapusta N (2008) Variability of earthquake nucleation in continuum models of rate-and-state faults and implications for aftershock rates. J Geophys Res 113:B12312. https://doi.org/10.1029/2007JB005154
Kato N (2004) Interaction of slip on asperities: numerical simulation of seismic cycles on a two-dimensional planar fault with nonuniform frictional property. J Geophys Res 109:B12306. https://doi.org/10.1029/2004JB003001

Kato N, Hirasawa T (2000) Effect of a large outer rise earthquake on seismic cycles of interplate earthquakes: a model study. J Geophys Res 105:653–662. https://doi.org/10.1029/1999JB900325
King GCP, Stein RS, Lin J (1994) Static stress changes and the triggering of earthquakes. Bull Seismol Soc Am 84:935–953
Li D, Liu Y (2016) Spatiotemporal evolution of slow slip events in a nonplanar fault model for northern Cascadia subduction zone. J Geophys Res 121:6828–6845. https://doi.org/10.1002/2016jb012857
Mitsui Y (2015) Interval modulation of recurrent slow slip events by two types of earthquake loading. Earth Planets Space 67:1–8. https://doi.org/10.1186/s40623-015-0230-2
Mitsui Y, Hirahara K (2011) Fault instability on a finite and planar fault related to early phase of nucleation. J Geophys Res Solid Earth 116:B06301. https://doi.org/10.1029/2010JB007974
Mitsui Y, Kato N, Fukahata Y, Hirahara K (2012) Megaquake cycle at the Tohoku subduction zone with thermal fluid pressurization near the surface. Earth Planet Sci Lett 325–326:21–26. https://doi.org/10.1016/j.epsl.2012.01.026
Nakano M, Hori T, Araki E et al (2018) Shallow very-low-frequency earthquakes accompany slow slip events in the Nankai subduction zone. Nat Commun 9:984. https://doi.org/10.1038/s41467-018-03431-5
Press WH, Teukolsky BP, Vetterling WT (1992) Numerical recipes, 2nd edn. Cambridge University Press, New York
Rani S, Singh SJ (1992) Static deformation of a uniform half-space due to a long dip-slip fault. Geophys J Int 109:469–476. https://doi.org/10.1111/j.1365-246X.1992.tb00108.x
Rice JR (1993) Spatio-temporal complexity of slip on a fault. J Geophys Res 98:9885–9907. https://doi.org/10.1029/93JB00191
Romanet P, Bhat HS, Jolivet R, Madariaga R (2018) Fast and slow earthquakes emerge due to fault geometrical complexity. Geophys Res Lett 45:4809–4819. https://doi.org/10.1029/2018GL077579
Rubin AM (2008) Episodic slow slip events and rate-and-state friction. J Geophys Res 113:B11414. https://doi.org/10.1029/2008JB005642
Rubin AM, Ampuero J-P (2005) Earthquake nucleation on (aging) rate and state faults. J Geophys Res 110:B11312. https://doi.org/10.1029/2005JB003686
Ruina A (1983) Slip instability and state variable friction laws. J Geophys Res 88:10359–10370. https://doi.org/10.1029/JB088iB12p10359
Segall P (2010) Earthquake and volcano deformation. Princeton University Press, Chicago
Tse ST, Rice JR (1986) Crustal earthquake instability in relation to the depth variation of frictional slip properties. J Geophys Res 91:9452–9472. https://doi.org/10.1029/JB091iB09p09452
Ujiie K, Kimura G (2014) Earthquake faulting in subduction zones: insights from fault rocks in accretionary prisms. Prog Earth Planet Sci 1:7. https://doi.org/10.1186/2197-4284-1-7
Veedu DM, Barbot S (2016) The Parkfield tremors reveal slow and fast ruptures on the same asperity. Nature 532:361–365. https://doi.org/10.1038/nature17190